Effects of carbon nanotube arrays on nucleate pool boiling

Sebastine Ujereh, Timothy Fisher, Issam Mudawar *

*Boiling and Two-Phase Flow Laboratory and Birck Nanotechnology Center, School of Mechanical Engineering, Purdue University,
West Lafayette, IN 47907, USA*

Abstract

Experiments were performed to assess the impact coating silicon and copper substrates with nanotubes (CNTs) have on pool boiling performance. Different CNT array densities and area coverages were tested on 1.27×1.27 mm^2 samples in FC-72. The CNT preparation techniques used provided strong adherence of CNTs to both substrate materials. Very small contact angle enabled deep penetration of FC-72 liquid inside surface cavities of smooth uncoated silicon surfaces, requiring unusually high surface superheat to initiate boiling. Fully coating the substrate surface with CNTs was highly effective at reducing the incipience superheat and greatly enhancing both the nucleate boiling heat transfer coefficient and critical heat flux (CHF). Efforts to further improve boiling performance by manipulating CNT area coverage of the substrate surface proved ineffective; best results were consistently realized with full surface coverage. Greater enhancement was achieved on silicon than on copper since, compared to uncoated copper surfaces, the uncoated silicon surfaces were very smooth and void of any sizeable nucleation sites to start with. This study is concluded with detailed metrics to assess the enhancement potential of the different CNT array densities and area coverages tested.
© 2007 Published by Elsevier Ltd.

1. Introduction

1.1. Rationale

In 1965 Gordon Moore proposed that the density of transistors on a chip will double every two years [1]. Corresponding to the tremendous enhancement in chip functionality realized with this trend has been a deleterious increase in the amount of heat generated per unit chip surface area. The quest for increasing more effective cooling schemes has therefore become a primary design concern throughout the microelectronics industry.

Air cooling schemes are still favored, where possible, for heat removal from electronic devices and systems. However, the effectiveness of such schemes has been compromised by the high heat fluxes of contemporary and projected high performance devices. Despite many innovative attempts to improve the heat removal capacity of air-cooling systems, including the use of massive fins and high-performance fans, the poor thermal transport properties of air limit their effectiveness. These limitations have shifted interest during the past two decades to the use of liquids to cool high-heat-flux devices. The obvious merit in this shift is the enormous cooling benefit realized with the superior thermal transport properties of liquid coolants.

Liquid cooling has been examined in a broad variety of flow configurations, including natural convection, channel flow, jet impingement and spray [2]. Each of these cooling configurations can be implemented with or without phase change. Overall, phase-change cooling schemes provide significantly superior cooling performance compared to their single-phase counterparts. However, they are generally more complex and more expensive to implement.

Of all the phase-change cooling schemes, natural convection boiling, more commonly referred to as pool boiling, is the simplest to implement. The most common cooling system utilizing pool boiling is a thermosyphon, which is essentially a closed system wherein vapor

---

* Corresponding author. Tel.: +1 765 494 5705; fax: +1 765 494 0539.
   E-mail address: im@mudawar.com (I. Mudawar).

Nomenclature

CHF	critical heat flux	σ	surface tension
h	heat transfer coefficient		
$h_{\max}$	maximum heat transfer coefficient	*Subscripts*	
q''	surface heat flux	f	liquid
T	temperature	g	vapor
ΔT_{sat}	surface-to-fluid temperature difference	max	maximum
		s	boiling surface
		sat	saturation
Greek symbols		∞	saturated liquid pool condition
λ_{T}	Taylor wavelength		
ρ	fluid density		

produced by boiling liquid on the device surface is separated by buoyancy. The vapor is collected in the upper portion of the system where it is returned to liquid state by condensation. The passive coolant circulation in a thermosyphon is central to the many advantages realized with this cooling scheme. Without a mechanical pump, thermosyphons are relatively inexpensive, quiet and reliable. Thermosyphons are therefore favored among all boiling schemes, provided they can satisfy the cooling requirements of high-flux devices.

While thermosyphons capitalize on the merits of boiling to dissipate the heat, their performance is limited by the low coolant flow rates induced in a stagnant liquid pool. High coolant velocities are central to the effectives of all other phase-change cooling schemes. Fewer options are therefore available for enhancing the cooling performance of a thermosyphon compared to those of other cooling systems. According to Anderson and Mudawar [3], heat transfer enhancement options in pool boiling are limited to (a) modifying the boiling surface, (b) subcooling the liquid to a temperature below the saturation temperature corresponding to the pool pressure, and/or (b) increasing the operating pressure. 'Enhancement of pool boiling' by surface modification is a phrase commonly used in the heat transfer literature that encompasses one or more of the following: (a) initiating nucleate boiling at a lower surface temperature, (b) reducing and/or eliminating the temperature overshoot and ensuing temperature drop corresponding to the inception of boiling (especially for low contact angle liquids, including most dielectric coolants), (c) reducing surface temperature (i.e., increasing the heat transfer coefficient associated with nucleate boiling), and (d) increasing the upper heat flux limit for nucleate boiling – critical heat flux (CHF) – in order to accommodate higher heat fluxes. The present study considers heat transfer enhancement by surface modification.

1.2. Pool boiling enhancement literature

Pool boiling heat transfer enhancement has been researched extensively over many decades. Both small- and large-scale modifications to the boiling surface have been shown to enhance pool boiling by reducing the surface temperature corresponding to boiling incipience, augmenting the nucleate boiling heat transfer coefficient, and delaying CHF. A book by Thome [4] provides a very comprehensive review of both the fundamental and practical aspects of boiling enhancement. Given the enormous number of articles and patents written on this subject, only a few representative and relevant studies are discussed here, with particular emphasis on low contact angle liquids such as those widely used in electronics cooling.

Enhancing the nucleate boiling heat transfer coefficient is commonly realized by modifying the boiling surface in pursuit of a greater number of nucleation sites per area [4]. On the other hand, CHF enhancement is commonly achieved by increasing boiling surface area using a variety of fin shapes and sizes [5,6]. Small-scale surface enhancement has been the focus of a growing number of studies spurred by recent improvements in the ability to create and characterize such surfaces. Nakayama et al. [7] showed that the rate of heat transfer from a porous surface to a dielectric coolant depends strongly on the number, size, and distribution of the pores.

Several commercially available surfaces have been tested in FC-72. These include porous sintered coatings (Union Carbide HIGH-FLUX), re-entrant grooves (Wielanderke AG GEWA-T), and tunneled surfaces formed by bending notched fins (Hitachi, THERMOEXCEL-E). Of these three surfaces, Marto and Lepere [8] showed that only the GEWA-T surface enhanced CHF for FC-72 compared to a smooth surface. This enhancement was attributed to increased surface area and the large spacing between re-entrant grooves, which resisted coalescence of vapor columns.

Anderson and Mudawar [5] showed that the surfaces with microgrooves and square microstuds are highly effective in enhancing the nucleate boiling heat transfer coefficient in FC-72 and increasing CHF by up to 2.5 times compared to a smooth surface. These enhancement effects were primarily the result of increased surface area. However, these surfaces exacerbated an incipience problem commonly encountered with low contact angle liquids.

These liquids have a tendency to penetrate deep inside surface cavities, requiring unusually high levels of superheat to initiate the boiling process.

In a follow-up study, Mudawar and Anderson [6] developed a three-level surface enhancement technique especially suited for low contact angle dielectric liquids. The first level was a centimeter-sized cylindrical stud that greatly increased heat transfer area. The second consisted of millimeter-sized fins that were machined along the circumference of the stud to further increase heat transfer area. The third enhancement level consisted of micronsized cavities that were formed by blasting the entire surface with a water-based slurry of 12,000 grit silica particles. This third level greatly increased the number of nucleation cavities per unit surface area. These types of surfaces were shown to eliminate the aforementioned incipience problem and enhance CHF by five and eight fold in saturated and subcooled FC-72, respectively.

Recently, Honda et al. [9,10] showed that silicon surfaces with nanoscale (25–32 nm) roughness yield better cooling with FC-72 than micro-pin-finned silicon surfaces in the lower heat flux boiling region. CHF values for the nano-roughened surface and micro-pin-finned surfaces were respectively 1.8 to 2.2 and 2.3 times those for smooth silicon.

1.3. Carbon nanotubes (CNTs)

The present study concerns the use of carbon nanotubes (CNTs) to enhance nucleate pool boiling. CNTs are extremely thin tubes of graphitic carbon with outer diameters ranging from 1 to 100 nm and lengths from 1 to 50 μm. Iijima [11] reviewed the recent trends and advancements in the understanding of these structures. CNTs take the form of single-walled nanotubes (SWNTs) or multi-walled nanotubes (MWNTs). SWNTs are made from a single graphene sheet, whereas MWNTs are made from multiple sheets. A graphene sheet consists of hexagonally arranged groups of carbon atoms. The discovery of CNTs generated great interest in the scientific community because their unique properties promise many applications. Most important among these properties are: mechanical strength superior to steel, density lower than aluminum, low-field electron emission, ultra-high electrical and thermal conductivity, needle-like structure, and thermal stability up to 1400 °C in vacuum. Possible applications of CNTs include flat panel displays (due to electron emission characteristics), probe tips (due to their needle-like structure), and various applications in electronics and thermal management that capitalize upon their excellent thermal conductivity and high mechanical strength.

Kim et al. [12] showed that the MWNTs can possess thermal conductivities in excess of 3000 W/m K at room temperature. This value is nearly eight times the conductivity of copper under similar conditions. This attribute renders CNTs very attractive for many demanding heat transfer applications.

1.4. Objectives of study

For a high-heat-flux surface that is coated with CNTs, very high thermal conductivity ensures that any added thermal resistance is small. Additionally, anchoring a mesh of billions of CNTs per square centimeter to the substrate surface is believed to greatly increase the number of bubble nucleation sites, thus both reducing the incipience temperature overshoot and increasing the nucleate boiling heat transfer coefficient during fully developed boiling. A unique feature of a CNT mesh is its three-dimensional structure, which provides an opportunity for capillary forces to route liquid laterally across the surface in order to maintain the boiling process during severe vapor effusion. This situation differs vastly from that of more conventional porous surfaces that only contribute increased nucleation site density. The CNT mesh is also believed to increase surface area corresponding to a very mild increase in volume, thus the potential for enhancing CHF compared to a bare surface. Given the aforementioned strong sensitivity of boiling behavior to even minute changes to surface microstructure, it is believed that CNT coating may have a profound effect on pool boiling performance.

The present study examines the effectiveness of CNTs in enhancing nucleate pool boiling by (a) capitalizing on their high thermal conductivity, (b) manipulating their anchoring, alignment and density on a substrate surface, and (c) modifying CNT coverage of the surface. The enhancement potential of CNTs is assessed by comparing the boiling performance of CNT-coated surfaces to those for bare surfaces. Results are presented for both silicon and copper substrates.

2. Experimental methods

2.1. Test heater construction

Experiments were performed to simulate chip heat dissipation and cooling. As shown in Fig. 1, heat was supplied from a 90 Ω thick film resistor that was soldered to the underside of an oxygen-free copper block. Two solder pads along opposite edges of the resistor were used to connect power lead wires to an external Variac. High-temperature solder (melting point of approximately 300 °C) attached the resistor to the copper block as well as the power leads to the resistor's pads. As shown in Fig. 2(a), different enhanced surface configurations took the form of a square chip (silicon or copper) that was adhered to the top surface of copper block, sealed circumferentially by a continuous bead of high-temperature RTV silicone rubber.

As shown in Fig. 2(a), the test heater was mounted in an assembly that provided thermal insulation along all sides of the copper block, insuring negligible heat loss from the test heater. The rate of heat dissipation from the test heater was therefore equal to the electrical power input to the resistive heater, which was measured by a Yokogama power meter. A K-type (Chromel–Alumel) thermocouple was embedded
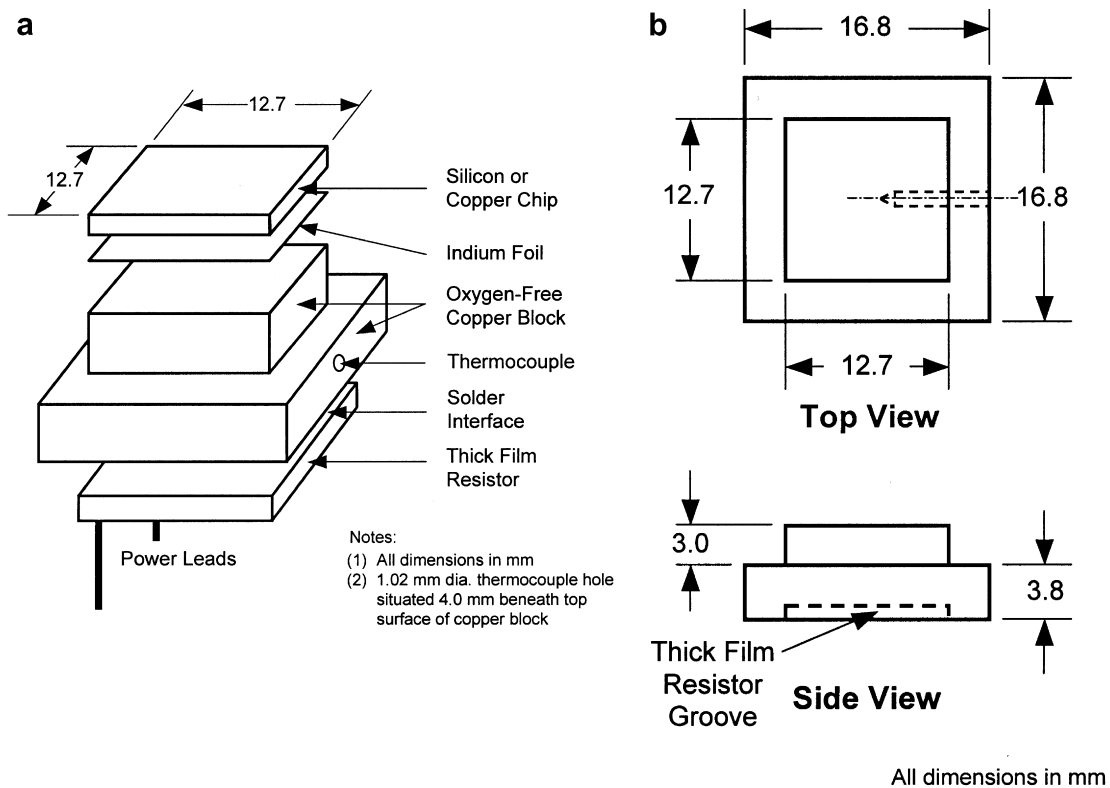
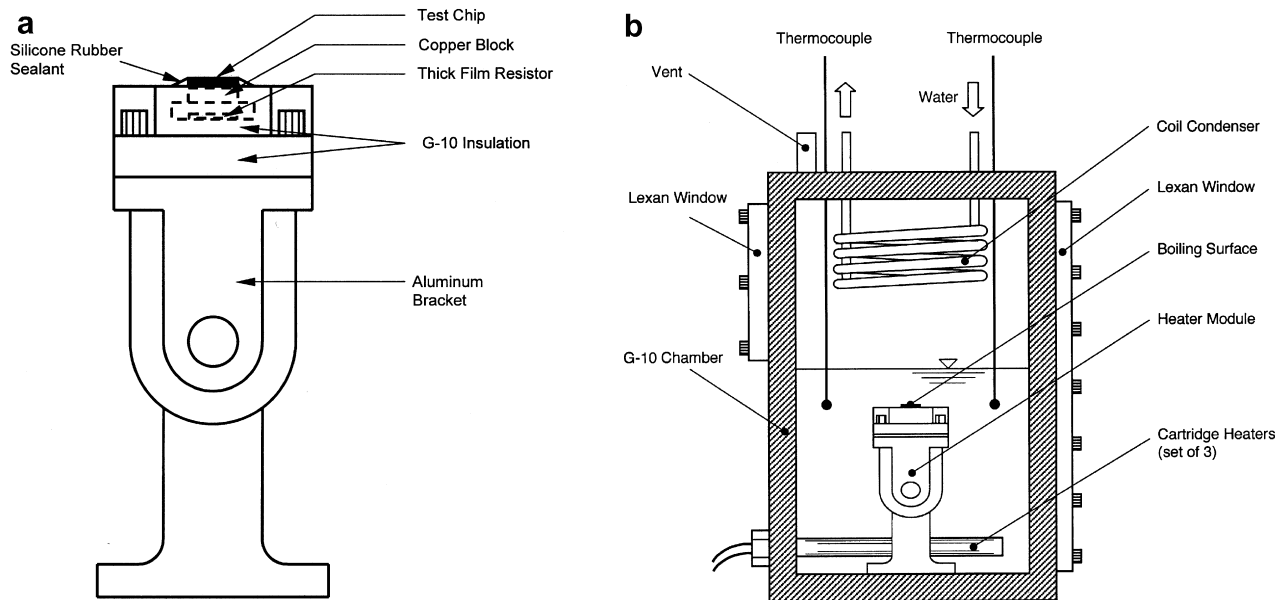Fig. 1. (a) Construction of a test heater. (b) Dimensions of copper heating block.

Fig. 2. Schematics of (a) heater module assembly and (b) boiling facility.

in the copper block to measure the block's temperature. The surface temperature, T_s, was extrapolated from the measured temperature by assuming one-dimensional conduction and a constant thermal conductivity (400 W/m K) for copper. Attaching a silicon or copper chip atop the copper block was accounted for by adding a thermal resistance corresponding to the thickness and conductivity of the chip and bonding medium.

Boiling performance in this study was investigated with the aid of plots of heat flux, q'', versus surface-to-fluid temperature difference, $\Delta T_{sat}(=T_s - T_\infty)$. The heat flux was calculated as the electrical power input divided by the top

area of the test chip, and T_∞ is the average of temperatures measured by two thermocouples immersed in the saturated liquid pool.

2.2. Test facility

After the enhanced surface was prepared, the test heater assembly was mounted to the bottom of a rectangular chamber as shown in Fig. 2. The chamber was filled with FC-72 liquid to a level several centimeters above the test chip. Cartridge heaters located at the bottom of the chamber were used to bring the FC-72 liquid to its saturation temperature and maintain it thereafter. These cartridge heaters were situated at the back of the chamber, separated from the bulk of the liquid pool by a metal plate, so as to preclude any natural convection currents or bubbles from influencing liquid motion in the vicinity of the test chip. Cooling water was supplied through a coil located in the upper portion of the chamber to condense the vapor generated during the tests.

The test heater and pool temperatures were measured and processed using a NI Daqpad 4350 interfaced to a NI TC 2190 thermocouple port made by National Instruments. The uncertainty in power supply is estimated to be 1% (device and measurement) and in thermocouple measurement is +/−0.5 °C. Heat loss is estimated at less than 5% of the electrical power input (see [13] for further details on heater construction and losses).

2.3. Operating procedure

Assessing the relative merits or drawbacks of a given surface required formulating and adopting a consistent operating procedure throughout the study. Tests began by filling the test chamber with two gallons of FC-72 at atmospheric pressure. Power to the pool's cartridge heaters was ramped to 90 W to preheat the liquid. After reaching its saturation temperature (56.6 °C), the liquid was allowed to boil vigorously for 45 min. to expel noncondensible gases. The cartridge heaters' power was subsequently reduced to 50 W to maintain saturated conditions. Concurrently, the power was supplied to the test heater to maintain fully developed boiling on the test surface for a few minutes before being reduced back to zero. This procedure helped to remove any air entrapped in the test surface itself during initial filling of the chamber.

Boiling tests commenced by increasing power input to the test surface in 0.5 W/cm^2 increments. Data were recorded between power increments after the test heater's thermocouple indicated that steady-state conditions had been reached within ±0.4 °C. Typical waiting periods to reach steady state ranged from 2 min. for lower heat fluxes to 5 min. near CHF. Incrementing power in this manner and recording steady-state temperature following each power increment enabled the generation of a boiling curve up to the CHF point. CHF was detected by a rapid, unsteady rise in the test heater's temperature. The power input was quickly reduced by about 1 W/cm^2 and then increased again in 0.2 W/cm^2 increments to obtain a more accurate CHF measurement. The power was then removed to prevent any damage to the test heater.

2.4. Carbon nanotube synthesis

To produce CNTs, a catalyst is required to initiate the growth of these microtubules of graphitic carbon. Several transition metals have been shown to produce CNTs; those most common are iron, cobalt, and nickel. In this study, all CNTs were produced using an iron catalyst because it yielded the most consistent and repeatable results.

Application of the catalyst to produce CNT growth can be achieved in several ways, depending on substrate material and CNT layout. In all cases a titanium under-layer was used. The present study capitalized on titanium's inherent ability to bond to other molecules in order to produce CNTs that are well anchored to a substrate. CNT anchoring is important for two reasons. First, well-anchored tubes facilitate minimal resistance to the heat transfer. Secondly, well-anchored CNTs are better able to withstand the vigor of the boiling process and help to maintain consistency and repeatability between tests.

2.4.1. Dendrimer catalyst sample preparation

Dendrimers are branched polymers that contain small voids capable of hosting minute quantities of other materials [14]. In the current work, processes described in [15] were employed to develop a dendrimer containing iron catalyst particles dispersed in these voids. This approach has been shown to improve the uniformity of CNT diameters [15] and to enable low-temperature synthesis [16].

0.42 g of a fourth-generation (G4) PAMAM (polyamidoamine) dendrimer with amine peripheral groups, made by Dendritic Nano Technologies, was dissolved in 20 mL of water. Separately, 0.5 g of $FeCl_3 \cdot 6H_2O$ (Aldrich) was dissolved in 20 mL of water. The two solutions were mixed and stirred vigorously for 2 h. A 30–100 nm titanium layer was deposited on the cleaned substrate using a Varian electron beam evaporator. The substrate was then dipped in the catalyst solution for various durations. The dendrimer was removed by mild calcination of the immobilized catalyst at 550 °C for 30 min to avoid passivation of the catalyst by the dendrimer. The calcination temperature was kept low to decrease the aggregation of the metallic clusters. The calcined catalyst was instrumental in the growth of CNTs in a plasma enhanced chemical vapor deposition (PECVD) system under optimal conditions.

2.4.2. Tri-layer metal catalyst sample preparation

A clean sample was placed in a Varian electron-beam metal evaporation system. 30 nm of titanium, 10 nm of aluminum, and 6 nm of iron were deposited in sequence on the bare substrate. Use of titanium and iron was discussed earlier. The purpose of the aluminum mid-layer was to prevent poisoning of the iron catalyst by the titanium, and also to

promote aggregation of the iron film into nanoparticles [17].

2.4.3. Plasma enhanced chemical vapor deposition (PECVD) system growth

The CNTs were grown in a PECVD system under conditions described by Maschmann et al. [18]. The conditions chosen for the iron catalyst include growth at 900 °C with a methane flow rate of 5–10 sccm (standard cubic centimeters per minute) and a hydrogen flow rate of 50 sccm. The process was run for 20 min to maximize CNT length and density on the substrate. The resulting CNT array is best described as a 'random mat' of MWNTs and not an ordered array.

2.5. Silicon boiling substrates

As in many prior electronic cooling studies, silicon was used as substrate to reproduce the thermal response of computer chips. This section describes the preparation of CNT coatings on a silicon substrate.

2.5.1. Bare silicon surface

Float zone silicon wafers were used for all tests involving silicon substrates. These double-side-polished silicon wafers have a diameter of 100 mm, a thickness of 400 μm, and a bulk resistivity in excess of 15,000 Ω-cm. The bare silicon substrates were formed by dicing the wafer into 12.7 mm × 12.7 mm square chips using a Tempress 602 dicing saw. As illustrated in Fig. 2(a), the square chip was adhered to the top surface of the copper heater block using 25 μm indium foil made by Honeywell. The thermal resistance introduced by this layer was measured previously [17] and was used to calculate the surface temperature as described above. Extreme care was exercised to ensure the silicon surface remained scratch-free throughout the adhesion process. Indium was quite effective for the purposes of the present study because of its malleability and ease of handling. In addition, indium's low melting point (156 °C) facilitated good adhesion by heating the test heater in a Lindberg Blue industrial oven preset to 175 °C. This simple indium adhesion technique eliminated the need for frequent handling of the silicon chip and furthered the end goal of protecting the surface from asperities. Furthermore, this technique ensured a consistent thickness of the adhesive layer.

2.5.2. CNT-coated silicon surface

A four-inch double-side-polished silicon wafer was diced into 12.7 mm × 12.7 mm squares. For the CNT-coated samples, a diamond-tipped scribe was used in place of the dicing saw to keep the silicon surface free from contaminants that may react with the CNT growth catalyst.

The titanium-coated chip was dipped in a dendrimer catalyst solution as described earlier to yield a CNT array with complete surface coverage. The CNT-coated silicon chip was then adhered to the top surface of copper heater block using indium foil. Once the CNTs were grown, and throughout the adhesion process, extreme care was exercised to avoid any damage to the CNTs, as even a brush with a fingertip might cause such damage. Fig. 3 shows a photograph of the CNT-coated silicon chip and scanning electron microscope (SEM) images of its surface. The resulting MWNTs are estimated to be approximately 50 nm in diameter and 20–30 μm long. These dimensions were consistent throughout the study; however, two different array densities were realized by altering the duration of submersion in the dendrimer solution between 12 and 24 h. The density of the primary ('light') CNT array is estimated to be 30 CNTs/μm². A second ('dense') CNT array had twice the density, 60 CNTs/μm². These density values are approximations based on analysis of the SEM images.

2.5.3. 'Grid' CNT pattern on silicon

Tests were conducted to explore the effects of partial coverage of the silicon surface with CNTs. Two CNT layouts were investigated: a 'grid' pattern, and an 'island' pattern. The 'grid' pattern's design was based on the Taylor instability wavelength [5],

$$\lambda_T = 2\pi \left[\frac{\sigma}{g(\rho_f - \rho_g)} \right]^{1/2}, \quad (1)$$

which is estimated at 5.0 mm for saturated FC-72 at one atmosphere. As shown in Fig. 4, the 'grid' array was sized to manipulate the Taylor wavelength to investigate whether this approach can delay in the onset of instability and therefore increase CHF. This effect will be discussed later.

The 'grid'-patterned chip was prepared using 3 M Kapton Tape. Initially, the tape fully covered the surface of a silicon chip. The tape was then cut to the pattern shown in Fig. 4 using a razor blade to expose the hatched pattern. Subsequently, the wafer was immersed in a dendrimer catalyst solution. CNTs were then grown on only the exposed surface as described earlier. The resulting CNT array density is estimated at 20 CNTs/μm².

2.5.4. 'Island' CNT pattern on silicon

The 'island' pattern was devised following preliminary experiments, which showed highly dense arrays of CNTs fully coated on a surface have adverse effects on heat transfer performance. The aim here was to create a CNT surface that is sparsely coated with CNT array clusters in order to further examine the effects of array surface coverage.

A shadow mask surface was created using a different catalyst application technique due to the size of the desired 'islands'. The catalyst was applied using the tri-layer metal evaporation technique described earlier. The shadow mask had 250 μm diameter holes with a uniform pitch of 1000 μm. The shadow mask was placed between the evaporating metal and the silicon substrate to produce the CNT catalyst 'islands' depicted in Fig. 5. Once again, the CNTs were synthesized using PECVD at standard conditions.
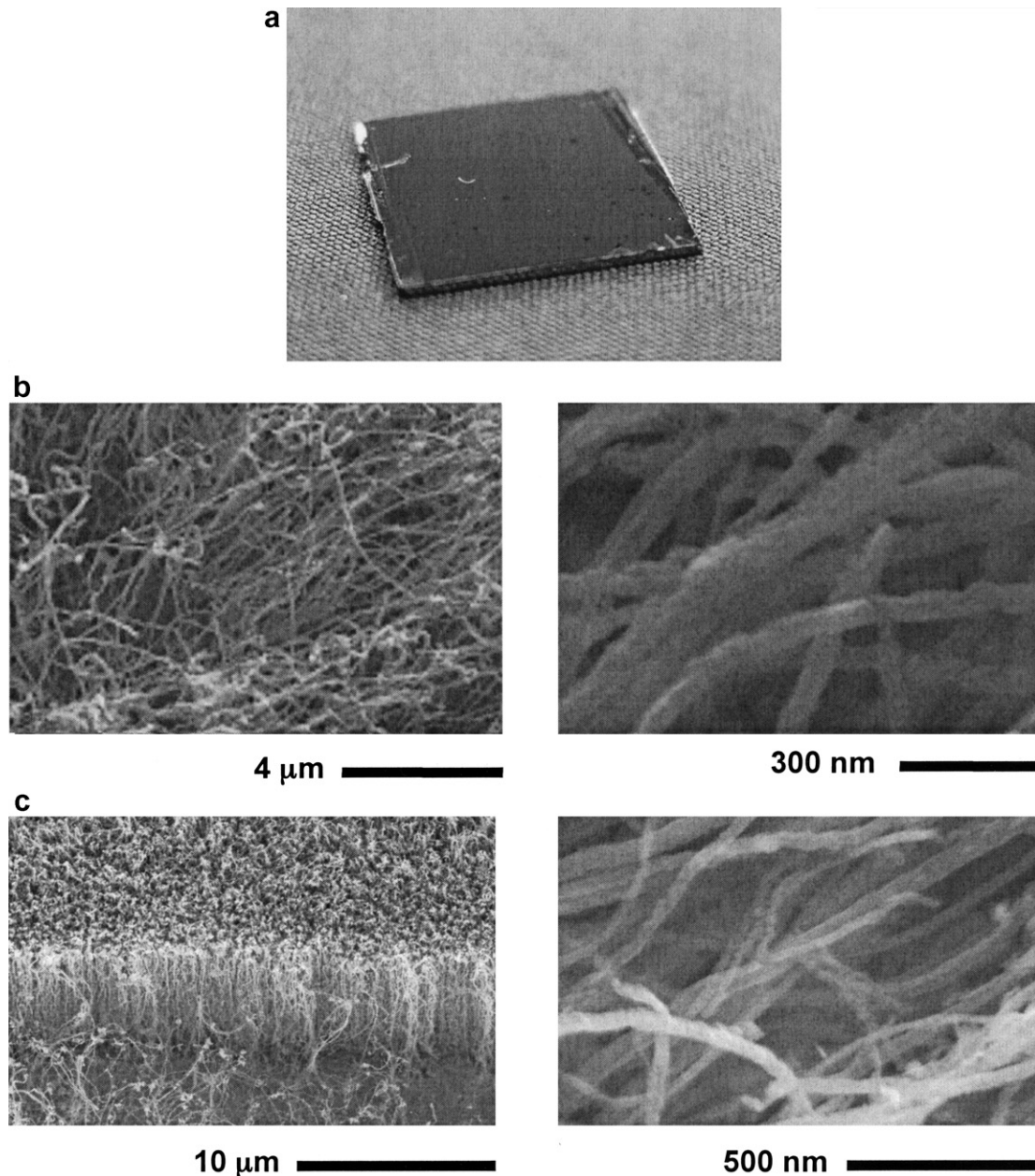
Fig. 3. (a) Photograph of silicon wafer and SEM images of silicon surface coated with (b) light CNT array and (c) dense CNT array.

The array density for this patterned substrate was approximately 20 CNTs/μm^2.

2.6. Copper boiling substrates

Copper is another important substrate material for chip cooling because it can be formed into complex finned surfaces that can be attached onto silicon chips. The aim in the present copper surface experiments was to investigate how CNTs may enhance boiling performance for both a flat copper surface as well as for a copper surface with micro-studs. We note that all CNT synthesis products on copper substrates shown below exhibit lower density and quality than those on silicon substrates. Possible explanations for this observation include catalyst contamination from diffu-sion of copper and surface roughness effects that affect catalyst particle aggregation during the growth process.

2.6.1. Flat copper surfaces

A bare copper surface served as reference for comparing the performances of the other copper surfaces. A copper chip was machined to the same size of the aforementioned silicon chips. The copper surface was then sanded with 400-grit sandpaper and cleaned thoroughly with methanol. Atomic force microscope (AFM) characterization revealed that the resulting surface possessed an abundance of 5–10 μm surface grooves.

A CNT-coated copper chip was formed by growing CNTs on a copper chip identical to the bare copper chip. In this case, a 30 nm titanium layer was first deposited on
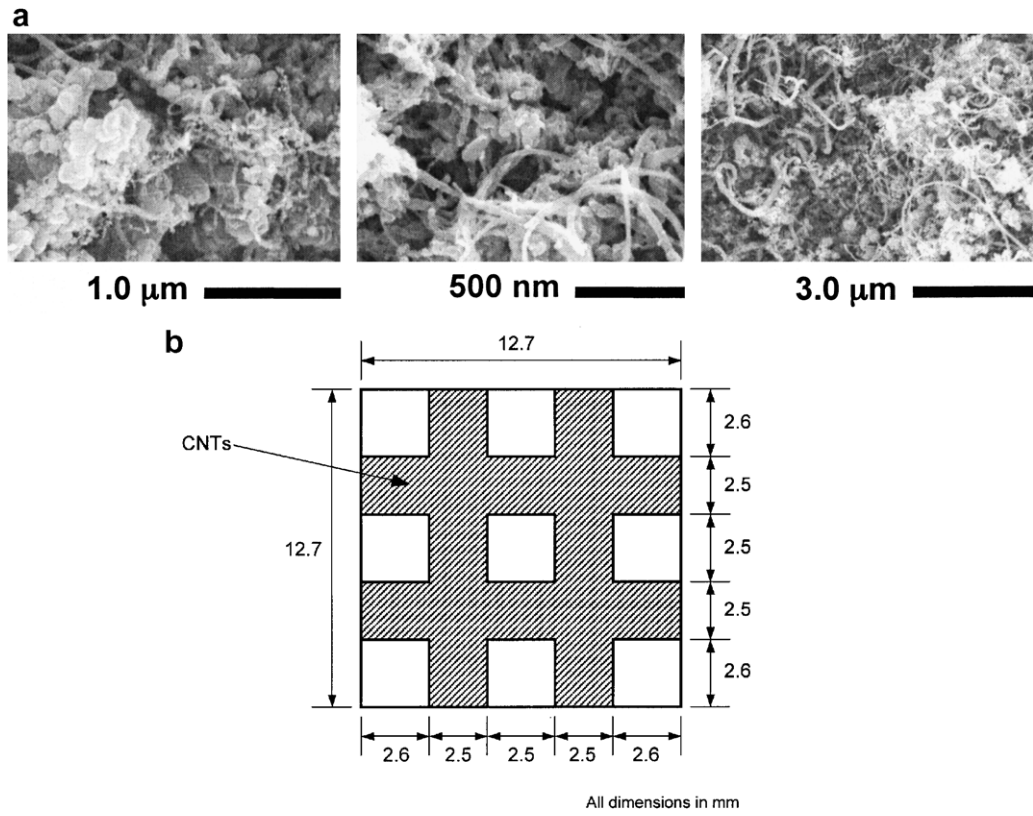
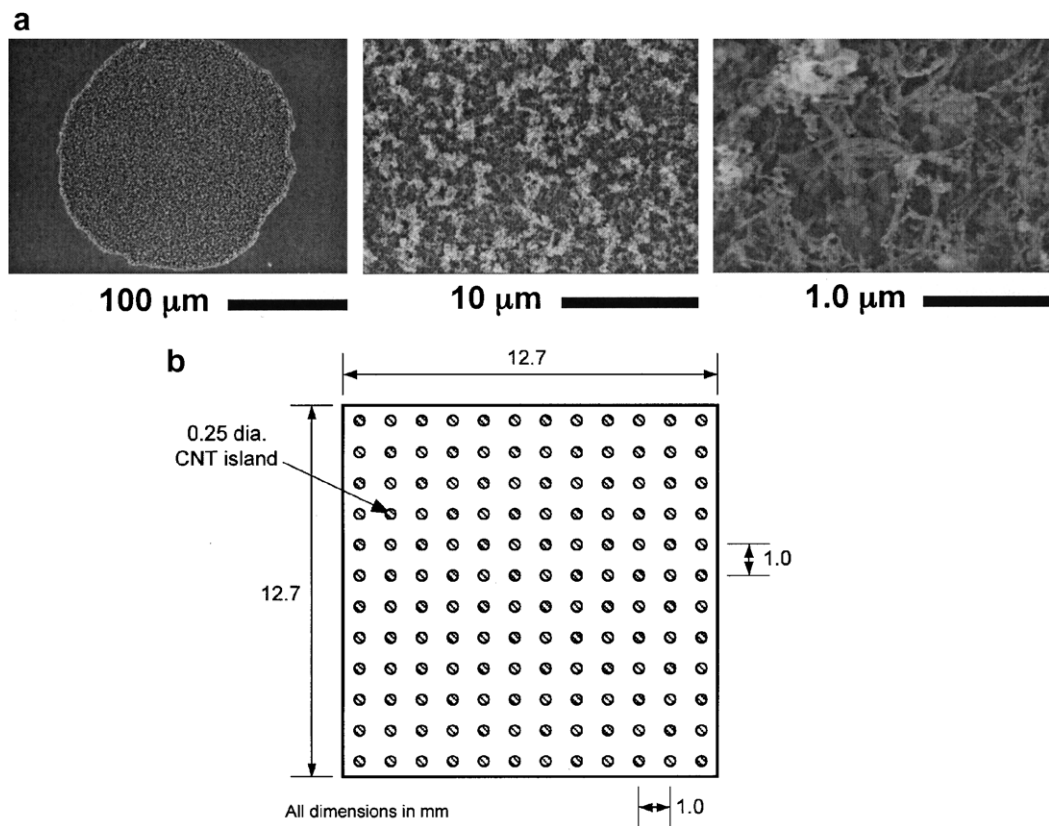Fig. 4. (a) SEM images and (b) CNT layout on 'grid'-patterned surface.

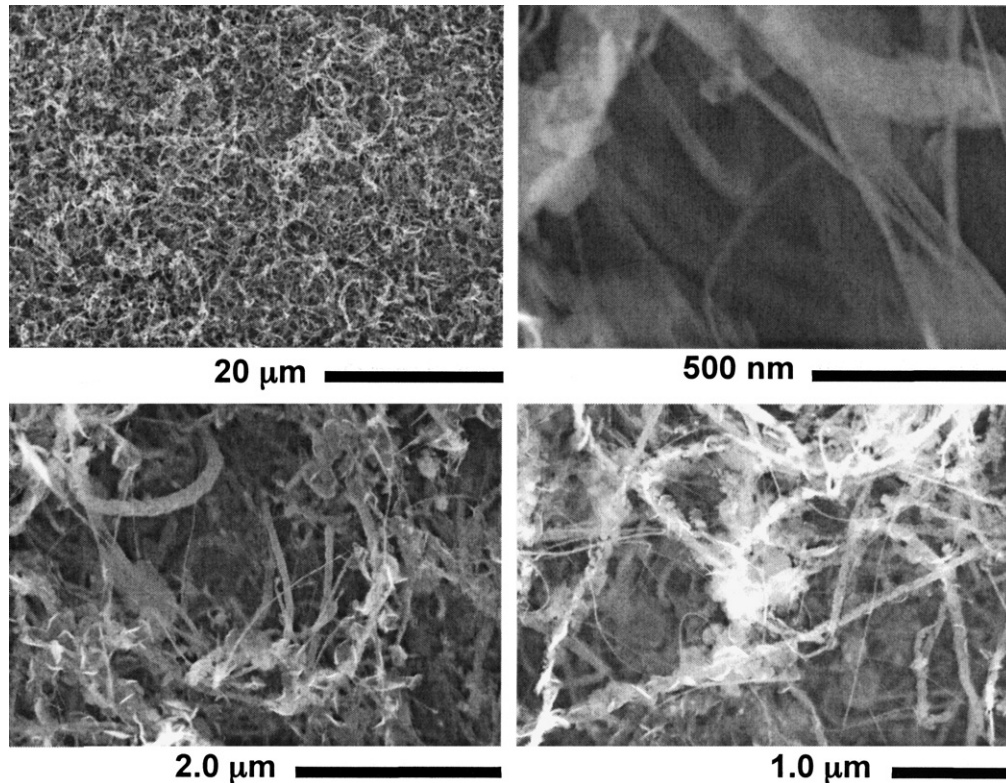Fig. 5. (a) SEM images and (b) CNT layout on 'island'-patterned surface.

Fig. 6. SEM images of CNT-coated flat copper surface.

the copper surface. A dendrimer catalyst was used to synthesize CNTs on the surface as described earlier. Fig. 6 depicts SEM images of the CNT-coated copper surface. The CNT array density for this surface is estimated to be $10 \, CNTs/\mu m^2$.

2.6.2. Microstud surfaces

Fig. 7a shows a schematic of a copper chip featuring an array of 0.25 mm square microstuds. This copper chip was adhered to the original copper heater block using indium foil.

CNTs were grown on the copper microstud surface using the tri-layer catalyst. The resulting surface is depicted in Fig. 7b. The array density for this surface is approximately $10 \, CNTs/\mu m^2$. It is important to note that the CNT catalyst application process precluded CNT growth along the circumference of the individual microstuds.

3. Experimental results

3.1. Boiling curve analysis parameters

Boiling curves were produced for different silicon and copper substrates. The boiling heat transfer coefficient, h, at any heat flux along the boiling curve was calculated as the ratio of heat flux to surface-to-fluid temperature difference, $q''/(T_s - T_\infty)$.

Several parameters were used to characterize the performance of a given surface. Boiling incipience superheat is the

wall superheat ($T_s - T_\infty$) corresponding to first bubble formation on the surface. Full nucleation coverage is defined as the lowest heat flux condition at which the surface became fully covered with nucleating bubbles. The fully developed pool boiling (FDB) superheat is defined as the surface-to-fluid temperature difference corresponding to full nucleation coverage. Another parameter that was used in assessing the merits of different surfaces is the maximum heat transfer coefficient, h_{max}, which is the largest heat transfer coefficient value determined along the entire boiling curve of a given surface. Lastly, surfaces were also rated based on critical heat flux (CHF) value.

3.2. Silicon substrate results

3.2.1. Bare silicon surface

The bare silicon surface served as the primary control for the boiling performance comparisons. Fig. 8 shows the results of the tests that were conducted with three separate but identical bare silicon samples. Overall, good agreement is evident in the single-phase natural convection region, the nucleate boiling region, and CHF. However, there are appreciable inconsistencies in the inception of boiling. Incipient temperature drop is nonexistent for surface A, mild for surface C and severe for surface B; differences in incipient superheat among the three surfaces are as high as 70%. This high degree of inconsistency is one of the key challenges facing the implementation of pool boiling in electronic cooling applications [5]. Two other challenges
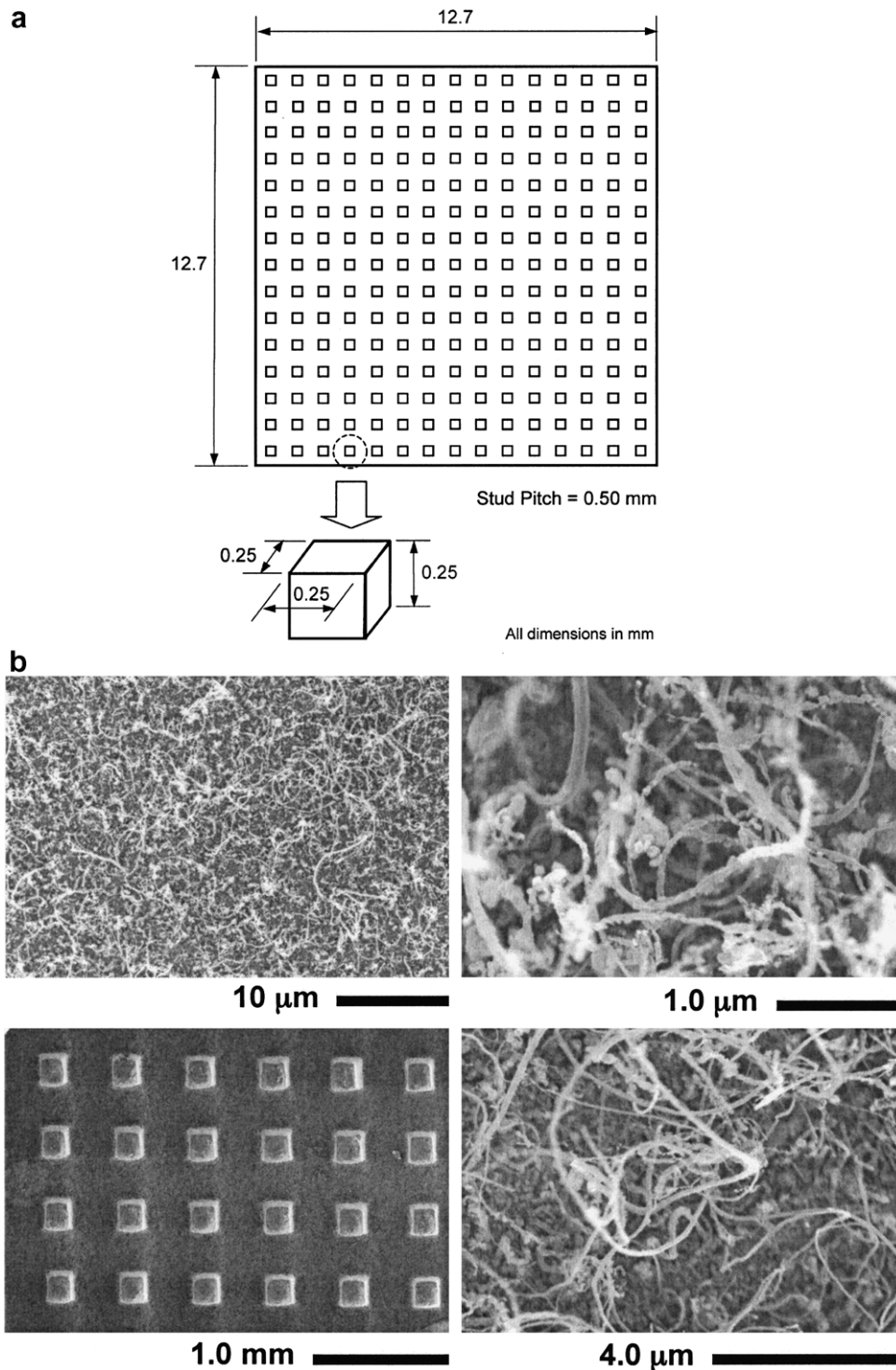
Fig. 7. (a) Dimensions of copper microstud surface. (b) SEM images of CNT-coated copper microstud surface.

are relatively high superheat in the nucleate boiling region and low CHF.

The large and often erratic boiling inception on bare silicon surfaces is problematic for two reasons. First, it may trigger large oscillations in chip temperature during chip power fluctuations. Second, a large incipient superheat can send a chip surface to temperatures far exceeding levels required for reliable chip performance. The large incipience

superheat is the result of both fluid properties and surface texture. Like all dielectric coolants, FC-72 has a very small contact angle on most surface materials. This allows FC-72 liquid to penetrate deep inside any available surface cavities, depriving the cavities from the sizable vapor embryos required to initiate boiling as surface temperature is slowly increased above saturation. The radius of curvature for any minute surface embryo that might form inside a cavity is
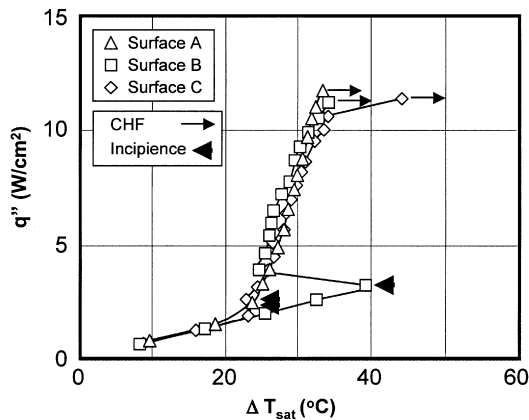
Fig. 8. Comparison of boiling curves for bare silicon surfaces.

quite small. The superheat required to grow an embryo beyond the mouth of a cavity is inversely proportional to the embryo's radius of curvature [4] and is therefore quite large for FC-72. While this behavior is true for FC-72 on most surfaces, it is especially problematic on a smooth silicon surface, which has very few sizeable cavities to start with. This means the difficulty initiating boiling in FC-72 is further exasperated on a smooth silicon surface.

3.2.2. CNT-coated silicon surface

A second series of experiments was conducted to explore the repeatability of boiling behavior on a fully CNT coated silicon surface, as well as to assess the impact of CNT density on boiling performance. Fig. 9 shows the results of two separate tests involving the 'light' CNT array (30 CNTs/μm^2) alongside those for the 'dense' CNT array (60 CNTs/μm^2). The two light array tests show good repeatability throughout the nucleate boiling region, with incipient superheats of 7.9 and 7.1 °C and corresponding CHF values of 18.1 and 17.1 W/cm^2. The dense array shows a noticeable decrease in the incipience superheat as well as a shift of the entire nucleate boiling region (2 °C at FDB) toward lower wall superheats. This heat transfer coefficient enhancement
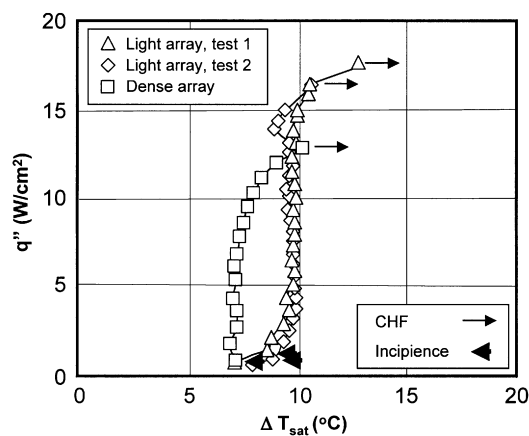
appears to be the result of the increased nucleation site density for the dense array. Notice, however, the inferior CHF value for the dense array. Referring to Fig. 3, it appears that the 'light' array provides greater accessible surface area compared to the more closely packed dense array. This may partially explain the superior CHF for the 'light' array. Clearly, array density yields conflicting performance effects. Optimum array density therefore depends on the primary purpose of the surface enhancement. It is important to note that no significant degradation of CNTs was observed in subsequent tests using the same fully CNT-coated silicon surface, suggesting that the CNTs were well anchored to the substrate.

Fig. 10a compares boiling curves for a fully CNT-coated silicon surface (light array test 1) and a bare silicon surface (sample A). The comparison reveals a 45% increase in CHF and a 67% decrease in incipience superheat for the CNT-coated surface. Furthermore, the maximum heat transfer coefficient for the CNT-coated surface is 18,200 W/m^2 K compared to only 3,300 W/m^2 K for bare silicon, a 450% enhancement. Based on visual observation, fully developed boiling for the bare silicon surface occurred at a superheat of 32 °C compared to only 10 °C for the CNT-coated surface. Fig. 10b shows images of the boiling surface for conditions indicated in Fig. 10a. Most noticeable is the inception of boiling on the CNT-coated surface at a much lower heat flux and lower superheat than the bare silicon.

These trends point to the effectiveness of CNTs at both initiating and sustaining the nucleation process. As indicated earlier, incipience with FC-72 is quite challenging on most surfaces, let alone a smooth silicon surface. The random mesh of CNTs appears to alter the vapor embryo entrapment process in several ways. This mesh includes patches of nearly vertical and parallel CNTs, other patches with nearly intersecting CNTs, and voids between CNTs and the different patches. Parallel CNTs create steep cavities with nearly zero effective cone angle. Such cavities are ideal for low contact angle liquids such as FC-72 since they have a tendency to trap vapor embryos regardless of contact angle. Intersecting patches of CNTs play a similar role by creating near zero cone angle cavities [19]. Finally, the voids act as 'reservoir-type' cavities that are ripe for nucleation with minimal superheat. In addition, the CNTs contribute significant surface area enhancement corresponding to only a minute increase in CNT volume. The high thermal conductivity of CNTs is believed to aid the utilization of surface area by facilitating extremely low resistance to conduction heat transfer. These combined effects may also explain the nearly vertical slope of the boiling curve for the CNT-coated surface. Such a slope is highly desirable in electronics cooling because it allows a chip to maintain a fairly constant temperature corresponding to relatively large fluctuations in heat dissipation during chip operation. Maintaining a constant chip temperature in this manner precludes thermal cycling in an electronic package and contributes to longer chip life and more reliable performance.
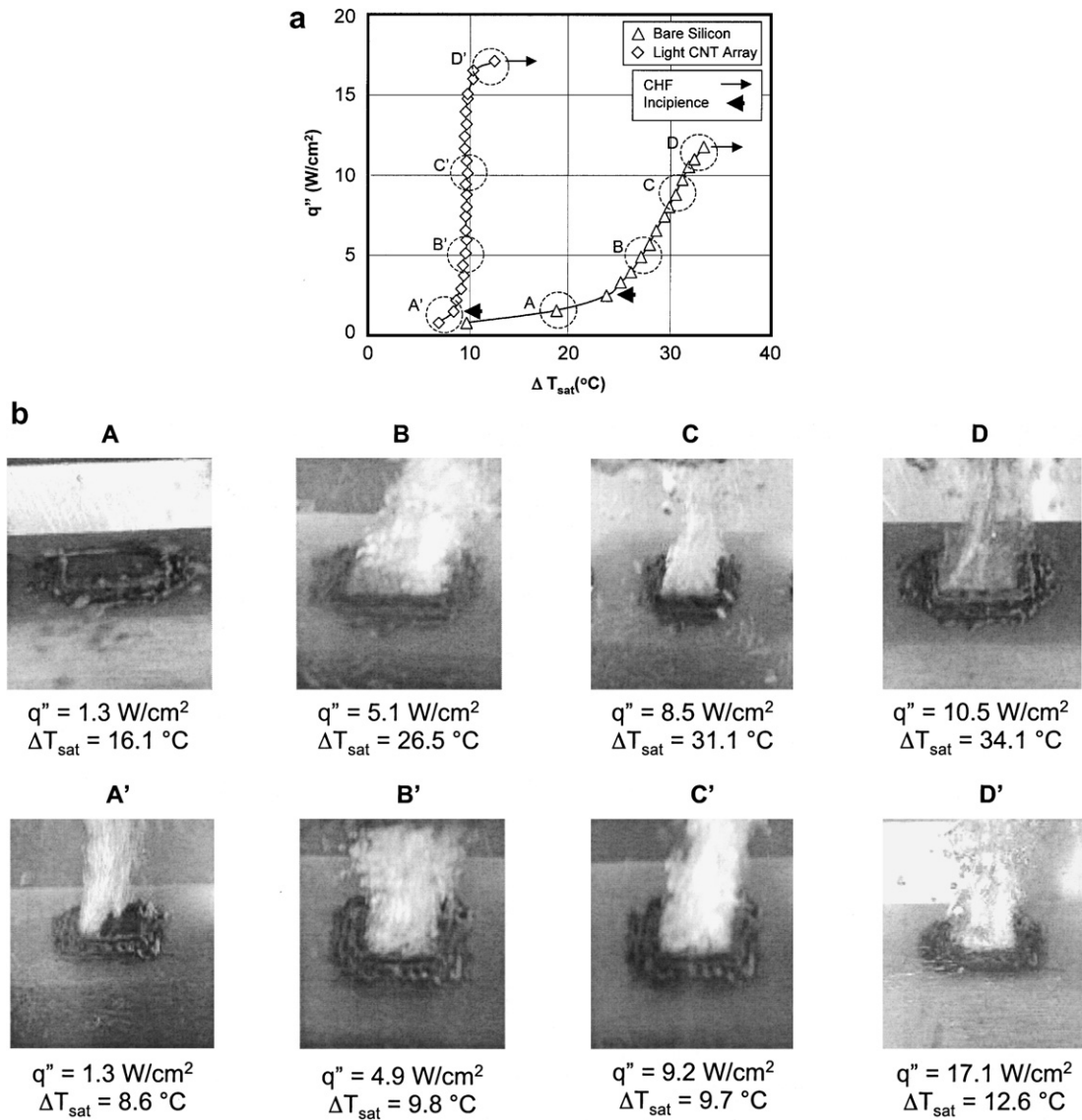

Fig. 9. Comparison of boiling curves for fully CNT-coated silicon surfaces.

Fig. 10. (a) Comparison of boiling curves for bare and fully CNT-coated silicon surfaces, and (b) corresponding boiling photographs.

3.2.3. 'Grid' and 'Island' CNT patterns on silicon

Two key parameters of CNT-coating are array density (as discussed earlier) and coverage of the chip's surface. To explore the effects of area coverage, boiling experiments were performed with silicon surfaces having the 'grid' and 'island' patterns shown in Figs. 4 and 5, respectively. Fig. 11 compares boiling curves for these two surfaces alongside those for the fully CNT-coated (light array) and bare silicon surfaces (sample B).

As discussed earlier, the 'grid' pattern was selected based on the Taylor instability wavelength and had CNT arrays covering approximately 60% of the total silicon substrate area. The width of the CNT grid is half the Taylor wavelength. The boiling incipience superheat with the 'grid' pattern is 12.7 °C, which is 46% lower than for bare silicon (sample A). The 'grid' surface also yielded a maximum heat transfer coefficient of 12,700 W/m² K, a 285% improvement over bare silicon. These results further confirm the
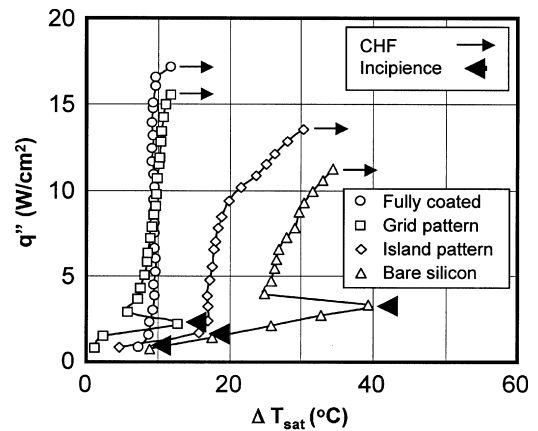

Fig. 11. Boiling curves for fully CNT-coated, CNT-patterned, and bare silicon surfaces.

effectiveness of CNT coating at enhancing nucleate boiling. Fig. 11 shows a slight incipient overshoot for the 'grid'

surface; however, upon incipience, 90% of the CNT surface was nucleating. Repeat experiments yielded similar results. CHF for the 'grid' surface was 15.8 W/cm^2, a 26% increase compared to bare silicon. This improvement is smaller than that realized with the fully CNT-coated silicon surface and is a clear indication that the attempt to enhance CHF by halving the Taylor instability wavelength did not yield the intended effect. Nonetheless, the array's effective heat transfer coefficient (slope of the boiling curve) is very similar to that for the fully coated surface. Further, this performance is realized with only 60% CNT surface coverage. Two consecutive boiling tests using the same 'grid' pattern showed a 67% difference in incipience superheat, followed in each case by a measurable temperature drop. This may be attributed to the existence of relatively large bare areas that resist nucleation. The two 'grid' pattern tests showed good repeatability in the nucleate boiling region with superheat values differing by less than 2% and a CHF difference of 5%.

The 'island' pattern provided approximately 5% CNT coverage of the total silicon surface area. This pattern also possessed light CNT array density. Fig. 11 shows an incipience superheat for this surface of 15.6 °C, and 18 °C superheat at full nucleation coverage. These values are, respectively, 34% and 44% lower than for bare silicon. The maximum heat transfer coefficient in this case is 4,562 W/m^2 K, a 38% increase compared to bare silicon. Finally, CHF occurred at 14.4 W/cm^2, which is 15% higher than for bare silicon. Similar to the 'grid' surface, the 'island' array showed no improvement in boiling performance metrics compared to the fully CNT-coated surface. Nonetheless, even with its minimal surface coverage (5%), the 'island' pattern yielded a substantial improvement in boiling performance compared to bare silicon. This is further evidence of the effectiveness of CNT arrays in general at enhancing pool boiling performance. However, results for the 'island' surface were somewhat less reproducible than for the 'grid' surface. This is evidenced by over 10% superheat differences in the fully developed boiling region and CHF differences in excess of 5%.

Overall, Fig. 11 shows a monotonic enhancement in both nucleate boiling heat transfer coefficient and CHF as CNT coverage of the silicon surface is increased from zero (bare surface) to 5% ('island' pattern), 60% ('grid' pattern), and ultimately to 100% (fully coated).

3.3. Copper substrate results

3.3.1. Bare and CNT-coated copper surfaces

Fig. 12 compares boiling results for the bare flat copper and CNT-coated copper surfaces. The incipience and fully developed boiling superheats for the CNT-coated copper surface are 8.4 and 8.7 °C, 40% and 37% smaller than bare copper, respectively. The maximum heat transfer coefficient and CHF are, respectively, 33% and 6% greater than for bare copper. Overall, the most impressive attribute of the CNT coating is the ability to sustain appreciably lower
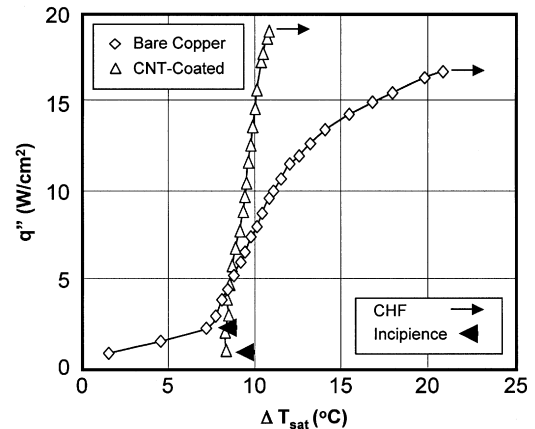

Fig. 12. Boiling curves for bare copper and fully CNT-coated copper surfaces.

superheats compared to bare copper even at conditions approaching CHF.

While these results do point to significant enhancement in heat transfer performance with CNT coating, this enhancement is less substantial than on silicon, as shown in Fig. 10. This observation may be explained by the initial roughness of the bare copper surface providing some enhancement compared to a bare silicon surface. The initial roughness was the result of pre-treating the bare copper surface with 400-grit paper. This treatment served to reduce both the incipience superheat and the superheat corresponding to fully developed boiling.

Tests were repeated for both the bare and CNT-coated copper surfaces. The bare surface showed significant variability in incipience superheat (more than 6 °C) and fully developed boiling superheat (over 48%). CHF values differed by only 4%. Conversely, the CNT-coated copper surface showed excellent repeatability, with variations between two tests of only 1% for the fully developed boiling superheat and less than 1% for CHF.

3.3.2. Uncoated and CNT-coated copper microstud surfaces

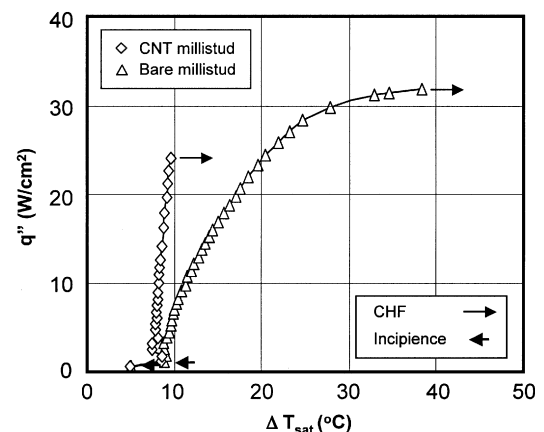Fig. 13 shows that CNTs greatly enhance the nucleate boiling performance of the microstud surface, but at the

Fig. 13. Boiling curves for bare and CNT-coated microstud surfaces.

Table 1
Summary of boiling metrics for different surfaces tested

	Surface	CHF (W/cm^2) (% change)	Incipience superheat (°C) (% change)	Fully developed boiling superheat (°C) (% change)	h_{max} (W/m^2 K) (% change)
Silicon					
Smooth silicon	Sample A	12.5	23.7	31.9	3,299
	Sample B	11.8	39.5	28.5	3,197
	Sample C	11.4	23.3	33.2	3,104
Fully CNT-coated silicon	Light array, test 1	18.1 (44.8%)	7.9 (−66.7%)	10.2 (−68.0%)	18,200 (452%)
	Light array, test 2	17.1 (36.8%)	7.1 (−70.0%)	9.3 (−77.9%)	15,732 (377%)
	Dense array, test 1	13.3 (6.4%)	7.2 (−69.6%)	8.4 (−73.7%)	12,376 (275%)
	Dense array, test 2	13.3 (6.4%)	7.9 (−66.7%)	8.3 (−74.0%)	13,348 (305%)
Patterned CNT on silicon	'Grid' array, test 2	15.8 (26.4%)	12.7 (−46.4%)	12.7 (−60.2%)	12,700 (285%)
	'Grid' array, test 1	15.0 (20.0%)	21.2 (−10.6%)	21.2 (−33.5%)	11,800 (258%)
	'Island' array, test 2	14.4 (15.2%)	15.6 (−34.2%)	18.0 (−43.6%)	4,562 (28.3%)
	'Island' array, test 1	13.6 (8.8%)	14.0 (−40.9%)	16.1 (−49.5%)	6,097 (84.8%)
Copper					
Bare copper	Test 2	18.4	13.9	13.9	13,200
	Test 1	17.7	7.2	7.2	9,540
Fully CNT-coated copper	Test 2	19.5 (6.0%)	8.4 (−39.6%)	13.9 (0%)	17,510 (32.7%)
	Test 1	19.4 (5.4%)	7.9 (−43.2%)	8.8 (−36.7%)	17,111 (29.6%)
Uncoated copper microstud	Test 2	32.3 (75.5%)	9.4 (−32.4%)	11.5 (−17.3%)	10,800 (−18.2%)
	Test 1	31.9 (73.4%)	9.1 (−34.5%)	10.6 (−23.7%)	11,900 (−9.9%)
CNT-coated copper microstud	Test 1	26.0 (41.3%)	5.5 (−60.4%)	9.0 (−35.3%)	26,500 (100.8%)
	Test 2	25.2 (37.0%)	5.1 (−63.3%)	9.0 (−35.3%)	23,930 (81.3%)

Comparisons for silicon surfaces are referenced to smooth surface sample A. Comparisons for copper surfaces are referenced to bare copper test 2. Reference conditions for each material are those that yielded the highest CHF value in repeatability tests.

expense of a noticeable (20%) reduction in CHF. Boiling incipience and fully developed boiling superheats were improved by 42% and 22%, respectively, and the maximum heat transfer coefficient by 145% over the uncoated microstud surface. The relatively poor CHF performance of the CNT-coated surface may be partially explained by the absence of CNTs along the circumference of the microstuds. Additionally, the thermal resistance of the copper microstuds themselves appears to reduce the effectiveness of the top CNT-coated surfaces of the microstuds compared to the CNT-coated base area between microstuds. Near CHF, the heat flow is biased to the CNT-coated base area, inducing severe vapor coalescence in the base region that engulfs the circumference and top surfaces of the microstuds.

Two separate tests with the uncoated microstud surface showed 8% deviation in fully developed boiling superheat and 1% difference in CHF. Repeatability tests with the CNT-coated microstud surface showed zero deviation in fully developed boiling superheat and 3% in CHF.

3.4. Summary of performance metrics

Table 1 provides a summary of boiling performance metrics for the different surface materials, CNT array densities and CNT area coverages tested in the present study. Performance parameters for different silicon tests are compared in absolute and percent change terms to those for

bare silicon. Similarly, copper tests are compared to bare copper. A clear trend emerges from this table. Excepting the fully-coated 'dense' CNT array case (which provided slightly lower superheat but lower CHF values than the fully-coated 'light' CNT array case), best *overall* results (lowest incipience superheat, lowest fully developed boiling superheat, highest boiling heat transfer coefficient, and highest CHF) were achieved by fully coating surfaces with a 'light' CNT array. Furthermore, the relative improvements are far more impressive for silicon because, as mentioned earlier, the reference uncoated silicon surface was very smooth and free of sizeable nucleation sites to start with.

4. Conclusions

This work has examined the effectiveness of carbon nanotubes (CNTs) in enhancing the pool boiling performance of low-contact-angle dielectric liquid FC-72 on silicon and copper surfaces similar to those used in the electronics industry. Such liquids pose several challenges to the implementation of pool boiling schemes, including large and erratic incipient boiling superheat and low CHF. Different CNT array densities and area coverages were tested to address these shortcomings. Boiling curves were generated to determine key performance metrics for different substrate materials and CNT patterns. Key findings from this study follow.

(1) The techniques developed in this study yield strong anchoring of CNTs to both silicon and copper substrates. This attribute was true for all CNT-coated surfaces tested and verifies by remarkable repeatability in boiling performance. Aside from minimizing resistance to heat transfer, these well-anchored CNTs appear fully capable of withstanding the vigor of the boiling process.

(2) Very small contact angle enables FC-72 liquid to penetrate deep inside surface cavities on uncoated surfaces, depriving the cavities from the sizable vapor embryos required to initiate the boiling. The small vapor embryos available deep inside the cavities require unusually high superheat. This problem is exacerbated on smooth silicon surfaces that possess very few sizeable cavities to start with. The large incipient temperature and ensuing temperature drop are completely eliminated when silicon and copper surfaces are fully coated with CNTs.

(3) Fully coating the substrate surface with CNTs is highly effective at both initiating and sustaining the nucleation process by altering the process of vapor embryo entrapment. The CNT mesh provides an abundance of zero cone angle and 'reservoir-type' cavities that are ripe for nucleation with minimal superheat. These combined effects may also explain the nearly vertical slope of the boiling curve, which is highly desirable in electronic cooling because it allows a chip to maintain a fairly constant temperature corresponding to relatively large fluctuations in heat dissipation during chip operation.

(4) Increasing CNT mesh density on silicon at the nanoscale reduces wall superheat slightly at incipience. However, highly dense CNT arrays also decrease CHF by reducing effective surface area. It is proposed that future research in which array density can be controlled and accurately evaluated should be investigated in optimizing both nucleate boiling wall superheat and CHF.

(5) Macroscale attempts to manipulate the CNT area coverage and layout on silicon proved ineffective in enhancing CHF. Overall, a monotonic enhancement was observed in both nucleate boiling heat transfer coefficient and CHF as CNT coverage of the silicon surface increased from zero (bare surface) to 5% ('island' pattern), 60% ('grid' pattern), and ultimately to 100% (fully coated).

(6) CNTs are quite effective in reducing incipience superheat and enhancing the boiling heat transfer coefficient for both bare and microstud enhanced copper surfaces. However, the enhancement is less than that realized on silicon because uncoated copper surfaces are rougher than uncoated silicon surfaces and therefore provide some initial enhancement to the boiling process. CHF with the CNT coating is slightly increased for bare copper but substantially decreased for the microstud surface. This decrease may be partially explained by the absence of CNTs along the circumference of the microstuds. Additionally, the thermal resistance of the copper microstuds appears to reduce the effectiveness of the top CNT-coated surfaces of the microstuds compared to the CNT-coated base area between microstuds. Near CHF, the heat flow is biased to the CNT-coated base area, inducing severe vapor coalescence in the base region that engulfs the circumference and top surfaces of the microstuds.

References

[1] G.E. Moore, Cramming more components onto integrated circuits, Electronics 38 (1965) 114–117.

[2] I. Mudawar, Assessment of high-heat-flux thermal management schemes, IEEE Trans.-CPMT: Components and Packaging Technologies 24 (2001) 122–141.

[3] T.M. Anderson, I. Mudawar, Parametric investigation into the effects of pressure, subcooling, surface augmentation and choice of coolant on pool boiling in the design of cooling systems for high-power-density electronic chips, ASME J. Electron. Packag. 112 (1990) 375–382.

[4] J.R. Thome, Enhanced Boiling Heat Transfer, Hemisphere Publishing Corporation, New York, NY, 1990.

[5] T.M. Anderson, I. Mudawar, Microelectronic cooling by enhanced pool boiling of a dielectric fluorocarbon liquid, ASME J. Heat Transfer 111 (1989) 752–759.

[6] I. Mudawar, T.M. Anderson, Optimization of enhanced surfaces for high flux chip cooling by pool boiling, ASME J. Electron. Packag. 115 (1993) 89–99.

[7] W. Nakayama, T. Daikoku, T. Nakajima, Effects of pore diameter and system pressure on saturated pool nucleate boiling heat transfer from porous surfaces, ASME J. Heat Transfer 104 (1982) 286–291.

[8] P.J. Marto, J. Lepere, Pool boiling heat transfer from enhanced surfaces to dielectric fluids, ASME J. Heat Transfer 104 (1982) 292–299.

[9] H. Honda, H. Takamastu, J.J. Wei, Enhanced boiling of FC-72 on silicon chips with micro-pin-fins and submicron-scale roughness, ASME J. Heat Transfer 124 (2002) 383–389.

[10] J.J. Wei, H. Honda, L.J. Guo, Experimental study of boiling phenomena and heat transfer performances of FC-72 over micro-pin-finned silicon chips, Heat Mass Transfer 41 (2005) 744–755.

[11] S. Iijima, Carbon nanotubes: past, present, and future, Physica B 323 (2002) 1–5.

[12] P. Kim, L. Shi, A. Majumdar, P.L. McEuen, Thermal transport measurements of individual multiwalled nanotubes, Phys. Rev. Lett. 87 (2001) 1–4.

[13] A.H. Howard, I. Mudawar, Orientation effects on pool boiling critical heat flux (CHF) and modeling of CHF for near-vertical surfaces, Int. J. Heat Mass Transfer 42 (1999) 1665–1688.

[14] R.M. Crooks, M. Zhao, L. Sun, V. Chechik, L.K. Yeung, Dendrimer encapsulated nanoparticles: synthesis, characterization, and applications to catalyst, Accounts Chem. Res. 34 (2001) 181–190.

[15] P.B. Amama, M.R. Maschmann, T.S. Fisher, T.D. Sands, Dendrimer-templated Fe nanoparticles for the growth of single-wall carbon nanotubes by plasma-enhanced CVD, J. Phys. Chem. B 110 (2006) 10636–10644.

[16] P.B. Amama, O. Ogebule, M.R. Maschmann, T.D. Sands, T.S. Fisher, Dendrimer-assisted low-temperature growth of carbon nanotubes by plasma-enhanced chemical vapor deposition, Chem. Commun. 27 (2006) 2899–2901.

[17] J. Xu, T.S. Fisher, Enhancement of thermal interface materials with carbon nanotube arrays, Int. J. Heat Mass Transfer 49 (2006) 1658–1666.

[18] M.R. Maschmann, P.B. Amama, A. Goyal, Z. Iqbal, R. Gat, T.S. Fisher, Parametric study of synthesis conditions in plasma-enhanced CVD of high-quality single-walled carbon nanotubes, Carbon 44 (2006) 10–18.

[19] S.J. Reed, I. Mudawar, Enhancement of boiling heat transfer using highly wetting liquids with pressed-on fins at low contact forces, Int. J. Heat Mass Transfer 40 (1997) 2379–2392.